Role of Interparticle Forces in the Formation of Random Loose Packing

K. J. Dong, R. Y. Yang, R. P. Zou, and A. B. Yu*

Center for Simulation and Modeling of Particulate Systems, School of Materials Science and Engineering,
University of New South Wales, Sydney, NSW 2052, Australia

(Received 3 November 2005; published 14 April 2006; corrected 17 April 2006)

We present a physical and numerical study of the settling of uniform spheres in liquids and show that interparticle forces play a critical role in forming the so-called random loose packing (RLP). Different packing conditions give different interparticle forces and, hence, different RLP. Two types of interparticle forces are identified: process dependent and process independent. The van der Waals force, as the major cohesive force in the present study, plays a critical role in effecting the process-dependent forces such as drag and lift forces. An equation is formulated to describe the relationship between the macroscopic packing fraction and microscopic interparticle forces in a packing. We argue there is no lowest packing fraction for a mechanically stable RLP; hence, the packing fractions of RLP can range from 0 to 0.64 depending on the cohesive and frictional conditions between particles.

DOI: 10.1103/PhysRevLett.96.145505 PACS numbers: 61.43.Gt, 61.43.Bn, 81.05.Rm

Two reproducible packing states have been identified for uniform spheres: random loose packing (RLP) and random close packing (RCP) [1,2]. They have been extensively studied and widely used to model the structure of liquids or amorphous solids and phase transition of colloidal systems [3–14]. Although well accepted, our knowledge about the nature and origin of the two states is still very limited. Traditionally, RCP is referred to as the densest state uniform spheres can achieve when randomly packed. Its packing fraction ρ_{RCP} is known as 0.6366 ± 0.0005 [2]. However, recent studies suggest that a slightly higher packing fraction is possible [8,9,13]. In particular, Torquato *et al.* [10] argued that RCP is ill defined and is better replaced by the so-called maximally random jamming state, which can be precisely defined. To date, the proof of their hypothesis is still open for research (see [15], for example).

RLP is even less well defined compared to RCP. It is generally referred to as the loosest, mechanically stable packing state of spheres. Its packing fraction ρ_{RLP} under gravity is around 0.60, slightly varying with packing conditions [1,2]. However, by settling glass spheres in liquids of different densities to neutralize the gravity force, Onoda and Liniger [16] obtained $\rho_{\mathrm{RLP}} = 0.555 \pm 0.005$. This packing fraction has since been widely accepted and is regarded to correspond to the dilatancy onset point or the transition from a liquid to a glassy state of hard sphere systems [6,7,16,17]. However, recent studies offer some results challenging the work of Onada and Liniger [11,17–22]. For example, Zhang *et al.* [19] showed that packing fraction ρ can be as low as 0.554 for cohesionless particles with high friction even when gravity is still dominant. On the other hand, when particles are nearly frictionless, O'Hern *et al.* [11] obtained $\rho = 0.639 \pm 0.001$, almost the same as ρ_{RCP}. For cohesive particles involving strong van der Waals and electrostatic forces, ρ decreases with particle size, approaching zero when the size is infinitely small [18,20]. All these results point to the fact that interparticle forces are important in producing RLP. Moreover, under the experimental conditions of Onada and Liniger [16], while the gravitational force is eliminated, there should be other liquid-related forces effected in their packing process [21,22]. These forces may interact with other forces and affect the final packing state. However, they are not considered in the work of Onada and Liniger [16].

Therefore, although RLP as a packing state has been widely used, there is a range of basic questions not properly answered yet. For example, what is RLP, in general? Is it a unique packing state of hard spheres? What is the role of interparticle forces in its formation? This Letter presents our answer to these questions.

Following the work of Onoda and Liniger [16], we formed a packing by settling spheres in a liquid by physical and numerical experiments. The numerical experiments were conducted by means of the so-called discrete element method (DEM) [23]. The DEM model in this work is similar to that in our study of the packing of fine particles in vacuum or air [18]. However, in addition to the contact and van der Waals forces considered there, three particle-fluid forces, namely, the buoyancy, drag, and Magnus lift forces, are also included. The equations to calculate these forces are well developed, given by [22,24,25]: $\mathbf{F}_{\mathrm{buoy}} = mg\rho_f/\rho_p$, $\mathbf{F}_{\mathrm{drag}} = \mathbf{f}_{f0,i}\varepsilon_i^{-(\eta+1)}$, and $\mathbf{F}_{\mathrm{lift}} = (\pi/8)\rho_f d_i^3(1-\varepsilon_i)[((1/2)\nabla\times\mathbf{u}_f - \boldsymbol{\omega}_i)\times(\mathbf{u}_f - \mathbf{u}_i)]$, where $\mathbf{u}_i$ and $\boldsymbol{\omega}_i$ are, respectively, the velocity and angular velocities of particle i. $\mathbf{u}_f$ and ε_i are, respectively, its surrounding fluid velocity and local porosity, $\mathbf{f}_{f0,i}$ is the drag force on an isolated particle, and η is the coefficient, depending on both the liquid properties and flowing conditions.

Table I lists the parameters used in this work. The particle properties are the same as those used in our previous work [14,18], which largely correspond to glass beads. Since the effects of particle properties have been examined elsewhere [19,26], this work is focused on the effects of liquid-related properties. For simplicity, unless

0031-9007/06/96(14)/145505(4)$23.00

otherwise specified, we vary such a property while the rest assume the default values.

A simulation starts with random generation of 3500 uniform sphere particles with no overlaps in a rectangular box of a length equal to $15d$. Periodic boundary conditions are applied to two horizontal directions to eliminate the so-called wall effect [14,18,27]. The particles are then allowed to settle down under the gravity and other forces mentioned above and form a stable packing when the velocities of all particles are essentially zero. Under the present experimental conditions, the motion of liquid is very small compared to that of particles. So, for simplicity, we ignore this motion in calculating the liquid-particle interactions. To determine the local porosity ε_i, the box is sliced vertically into sections of height $1.5d$, and the porosity of each section is calculated and assigned to the particles whose centers are in the section.

To validate the numerical model, physical experiments are also conducted under comparable conditions. This is done by settling narrowly sized glass beads, which are 110 ± 4, 250 ± 9, or 500 ± 20 μm, in a solution of diiodomethane ($\rho_f = 3300$ kg/m^3 and $\mu_f = 0.0035$ kg/ms) and toluene ($\rho_f = 867$ kg/m^3 and $\mu_f = 0.000\,59$ kg/ms). Liquid density can be adjusted by altering liquid composition as done by Onada and Liniger [16]. However, it should be noted that not only liquid density but also viscosity vary with liquid composition. The former varies linearly with liquid composition as theoretically expected for well mixed solutions, and the latter is measured by using a viscosity meter (the results shown in Fig. 1).

The van der Waals force is calculated according to the equation for smooth spheres [18]. In the equation, the so-called Hamaker constant is the only unknown parameter. Theoretically speaking, this constant depends on many variables related to physical and chemical properties, such as particle surface roughness or asperity, medium chemistry, and so on [28]. It is difficult to evaluate the effects of these variables comprehensively. In numerical modeling, this constant is often treated as a lumped parameter and determined empirically. For this work, we use a simple method to determine its value. Knowing the Hamaker constants of toluene (4.0×10^{-21} J), diiodomethane (7.1×10^{-21} J), and glass beads (6.5×10^{-21} J) in vacuum, we first estimate the Hamaker constant of glass beads in pure toluene and diiodomethane, 3.0×10^{-21} and 1.0×10^{-22} J, respectively, according to $A_{121} \approx (\sqrt{A_1} - \sqrt{A_2})^2$, where A_1 and A_2 are, respectively, the Hamaker constants of materials 1 and 2 in vacuum, and A_{121} is the Hamaker constant of material 1 in (medium) material 2 [28]. The Hamaker constant of glass beads in a liquid solution is then obtained as the weighted mean of the two resulting Hamaker constants according to the molar weights of toluene and diiodomethane.

Figure 1 shows ρ as a function of the effective gravitational acceleration Δg $[=(1 - \rho_f/\rho_p)g]$. Onoda and Liniger [16] adopted the same plot for 250 μm glass beads. Their results are also included in Fig. 1 for comparison. Clearly, our experimental results are comparable to theirs. The extrapolation of ρ when $\Delta g \rightarrow 0$ also suggests $\rho = 0.555$. However, such an extrapolated ρ is not constant but varies with particle size d. In fact, it equals 0.505 or 0.585 for 500 or 110 μm glass beads. This fact indicates that the RLP produced by Onoda and Liniger is not unique, and packing conditions are important in producing RLP. It can also be seen from Fig. 1 that the DEM can reasonably reproduce the experimental results for all sized particles, confirming the validity of the proposed simulation technique.

We then quantified the effects of individual variables related to material properties by conducting a series of numerical experiments, which are difficult to realize in physical experiments because the variables are often coupled as seen above. Figure 2 shows the effects of Hamaker constant A, particle size d, liquid density ρ_f, and liquid viscosity μ_f on packing density ρ. Figure 2(a) demonstrates that ρ decreases with increasing A, which is qualitatively consistent with the previous findings [26]. However, quantitatively, the decrease is more significant in heavier liquids. This is because increasing A will increase the van der Waals force, which restricts the relative

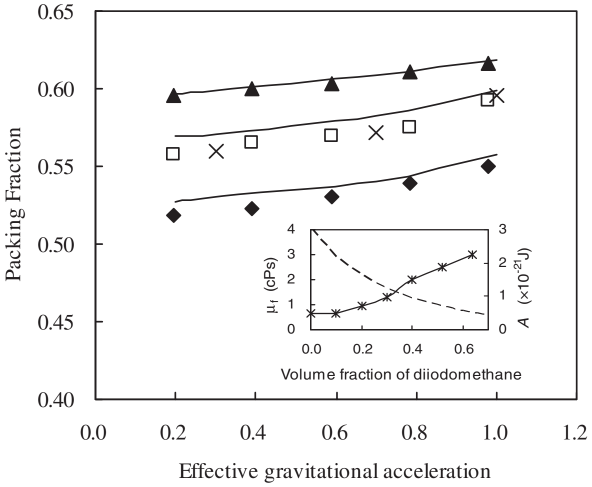

FIG. 1. The packing fraction of different sized glass beads as a function of the effective gravitational acceleration. Points are the measured results: ▲, $d = 500$ μm; □, $d = 250$ μm; ◆, $d = 110$ μm; and ×, results of Onoda and Liniger [16]. Lines are the simulated results. The inset shows the variation of viscosity (solid line) and the Hamaker constant (dashed line) with liquid composition.

TABLE I. The parameters used in the simulation.

Parameter	Default and varying range (bracketed)
Particle size d	250 μm (5–1000)
Particle density ρ_p	2460 kg/m^3 (constant)
Liquid density ρ_f	1000 kg/m^3 (500–2450)
Liquid viscosity μ_f	0.001 238 kg/ms (0.0001–0.1)
Hamaker constant A	6.5×10^{-20} J (1.0×10^{-22}–1.0×10^{-19})

motion between particles, and an increased ρ_f means a decrease in the effective gravity, which drives particles to settle down to form a stable packing. Increasing d can increase this driving force and, hence, ρ. However, if d is greater than a certain value, geometrical constraints become dominant, leading to an essentially constant ρ for a given packing condition. For the packing of particles in vacuum or air, the effect of d has been well established in the literature [18,29]. Figure 2(b) shows that packing particles in liquids gives the same trend. However, because of the change in the interparticle forces, the packing results quantitatively differ. In particular, the effect of d can be extended to a larger size range.

Increasing ρ_f or μ_f will decrease ρ, because the former decreases the driving force, while the latter increases the force resistant to the motion of particles. The results in Figs. 2(c) and 2(d) indicate that this effect becomes more and more significant as the difference between ρ_p and ρ_f or d decreases or μ_f increases. This must be related to the change in the relative importance among the forces governing the motion of particles. The results also explain why liquid-related forces can usually be ignored when particles are packed in air, because it has a negligible ρ_f and μ_f.

One important finding from Fig. 2 is that the van der Waals force $\mathbf{F}_{\mathrm{vdw}}$ is critical to the performance of other forces. Without this force (when $A = 0$), d, ρ_f, or μ_f has little effect on ρ. In this case, $\rho = 0.615$, which corresponds to the case when glass beads settle down under gravity. Changing the material properties, interparticle friction in particular, results in a change in ρ [26,30]. Interestingly, when frictionless spheres are used, achieved by assuming sliding and rolling friction coefficients both equal to zero, ρ would be 0.64. That is, for cohesionless and frictionless spheres, RLP is the same as RCP, as discussed by O'Hern *et al.* [11]. Moreover, our simulation indicates this value is not affected by the value assigned to Δg.

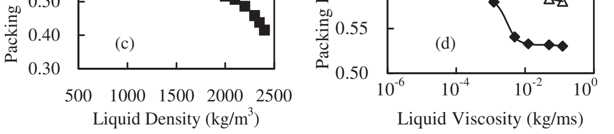

FIG. 2. The packing fraction as a function of: (a) the Hamaker constant when $\rho_f = 2200$ kg/m^3 (◆) and $\rho_f = 2400$ kg/m^3 (□); (b) particle size when $A = 6.5 \times 10^{-20}$ J and $\rho_f = 0$ (▲) or 1000 kg/m^3 (◆), and $A = 0$ J and $\rho_f = 1000$ kg/m^3 (□); (c) liquid density when $A = 6.5 \times 10^{-20}$ J and $d = 1000$ (◇) or $d = 250$ μm (■), and $A = 0$ J and $d = 250$ μm (×); (d) liquid viscosity when $A = 6.5 \times 10^{-20}$ J and $d = 1000$ (△) or $d = 250$ μm (◆), and $A = 0$ J and $d = 250$ μm (×). The default values listed in Table I are used for unspecified parameters.

Associated with the change in macroscopic properties such as packing fraction is the change in microscopic properties. We have determined structural parameters such as radial distribution function, coordination number, and some topological and metric properties as done elsewhere [14,18,26] and found that the results are comparable when the packing fraction decreases with the decrease of d or the increase of ρ_f and/or μ_f, indicating various material properties affect particle packing by the same mechanisms. Such mechanisms, if available, must be directly related to the forces controlling the packing process. For the considered system, the forces include contact, noncontact, and liquid-related forces, in addition to gravity. As contact forces have been discussed elsewhere [26], we focus on liquid-related forces here. Figure 3 shows the evolution of the averaged forces acting on individual particles in a settling process. Once the settling process starts, particles quickly reach their terminal velocity and gain the maximum drag force from the liquids. The interaction between particles initiates the lift and van der Waals forces. Once particles reach the packing formed by the underneath particles, they will rearrange themselves. During this period, the drag and lift forces decrease and eventually vanish when particles have negligible velocities. On the contrary, the van der Waals force increases to its maximum and then becomes constant.

The forces can be classified into two categories: process dependent and process independent. The first category includes the drag, lift, and van der Waals forces. It is clear from Fig. 3 that the first two will disappear and the last one reaches its maximum constant once a stable packing is formed. The second category includes the buoyancy and gravitational forces. These two forces are constant, independent of the settling process. It has been found that, for cohesive particles packed in air or vacuum under gravity, the packing fraction can be related to the ratio of the magnitudes of the van der Waals force to the gravity [18,20]. For packing in liquid, the gravity force can be

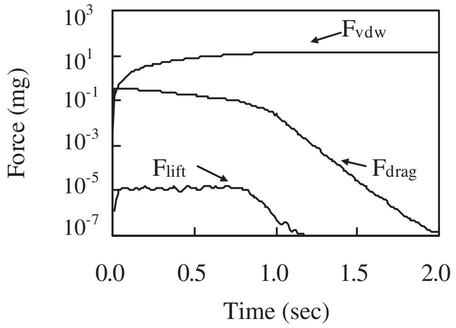

FIG. 3. Evolutions of the averaged process-dependent forces $|\mathbf{F}_{\mathrm{vdw}}|$, $|\mathbf{F}_{\mathrm{drag}}|$, and $|\mathbf{F}_{\mathrm{lift}}|$ with time.

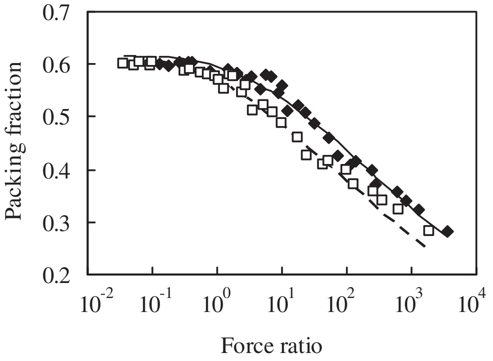

FIG. 4. The packing fraction as a function of the force ratio between the averaged van der Waals force and effective gravity acting on individual particles in a packing: ◆, χ'; and □, χ.

replaced by the effective gravity force. That is, the force ratio can be given as: $\chi = |\sum_j \mathbf{F}_{ij}^{\nu}|/m\Delta g$ or $\chi' = \sum_j |\mathbf{F}_{ij}^{\nu}|/m\Delta g$. Note that this force ratio is similar to the so-called Bond number defined as $|\mathbf{F}_{ij}^{\nu}|$/mg and found to be useful in describing the dynamic behavior of cohesive powders [31,32]. However, in our treatment, the cohesive forces considered are related directly to the packing structure, different from that measured under conditions which are not necessarily associated with any structure.

Figure 4 plots ρ as a function of χ or χ'. It confirms the validity of equation $\rho = \rho_0(1 - \exp(\alpha\chi^{\beta}))$, where ρ_0 is the packing fraction of cohesionless spheres, and α and β are parameters relating to particle properties [18,26]. For frictionless particles, $\rho_0 = 0.64$, the same as ρ_{RCP} as discussed earlier. For frictional particles, ρ_0 varies and can be as low as 0.554 [19]. Here we obtained $\rho_0 = 0.616$, and, for χ, $\alpha = -2.457$ and $\beta = -0.212$; for χ', $\alpha = -3.235$ and $\beta = -0.271$. These results are very similar to those obtained by Yang *et al.* [18] for the packing of cohesive particles in vacuum. This equation also applies to other cohesive forces such as the capillary force [20]. It can therefore be used as an equation of state to describe the relationship between the macroscopic packing fraction and the microscopic interparticle forces in a packing [22]. It suggests that, when the force ratio is infinitely large, ρ is zero. Indeed, a packing fraction as low as 0.01 has been observed for nanoparticles [29,33].

In summary, we have studied the settling of particles in liquids and shown that interparticle forces play a critical role in forming RLP by this commonly used technique. The RLP generated by Scott and Kilgour [2] or Onoda and Liniger [16] is not unique. Different packing conditions give different interparticle forces and, hence, different RLP. Two types of interparticle forces have been identified: process dependent and process independent. Focused on the final packing state, we show that the packing fraction can be related to the force ratio between cohesive force and effective gravity. This correlation can act as an equation of state to describe the relationship between the macroscopic packing fraction and the microscopic interparticle forces in a packing. For the system considered, the van der Waals force, as the major cohesive force, plays a critical role in effecting the process-dependent, liquid-related forces such as drag and lift forces. For cohesive particles, the packing fraction of RLP can range from 0 to 0.64. For cohesionless particles, it may vary with material properties such as friction coefficients in a narrower range, probably from 0.554 to 0.64. For cohesionless and frictionless particles, it is the same as RCP, equal to 0.64.

We are grateful to the Australian Research Council for the financial support of this work.

---

*Corresponding author.
Electronic address: a.yu@unsw.edu.au

[1] G. D. Scott, Nature (London) **188**, 908 (1960).
[2] G. D. Scott and D. M. Kilgour, J. Phys. D: Appl. Phys. **2**, 863 (1969).
[3] J. D. Bernal, Proc. R. Soc. A **280**, 299 (1964).
[4] K. Gotoh and J. L. Finney, Nature (London) **252**, 202 (1974).
[5] F. H. Stillinger and T. A. Weber, Science **225**, 983 (1984).
[6] P. N. Pusey *et al.*, Phys. Rev. Lett. **63**, 2753 (1989).
[7] J. Zhu *et al.*, Nature (London) **387**, 883 (1997).
[8] O. Pouliquen *et al.*, Phys. Rev. Lett. **79**, 3640 (1997).
[9] E. R. Nowak *et al.*, Phys. Rev. E **57**, 1971 (1998).
[10] S. Torquato *et al.*, Phys. Rev. Lett. **84**, 2064 (2000).
[11] C. S. O'Hern *et al.*, Phys. Rev. Lett. **88**, 075507 (2002).
[12] C. S. O'Hern *et al.*, Phys. Rev. E **68**, 011306 (2003).
[13] K. E. Daniels and R. P. Behringer, Phys. Rev. Lett. **94**, 168001 (2005).
[14] X. Z. An *et al.*, Phys. Rev. Lett. **95**, 205502 (2005).
[15] A. R. Kansal *et al.*, Phys. Rev. E **66**, 041109 (2002).
[16] G. Y. Onoda and E. G. Liniger, Phys. Rev. Lett. **64**, 2727 (1990).
[17] A. P. Shapiro and R. F. Probstein, Phys. Rev. Lett. **68**, 1422 (1992).
[18] R. Y. Yang *et al.*, Phys. Rev. E **62**, 3900 (2000); **65**, 041302 (2002).
[19] Z. P. Zhang *et al.*, Powder Technol. **116**, 23 (2001).
[20] A. B. Yu *et al.*, Powder Technol. **130**, 70 (2003).
[21] S. C. Pont *et al.*, Phys. Rev. Lett. **90**, 044301 (2003).
[22] A. B. Yu, *Encyclopedia of Condensed Matter Physics* (Elsevier, New York, 2005), Vol. 4, pp. 401–414.
[23] P. A. Cundall and O. D. L. Strack, Geotechnique **29**, 47 (1979).
[24] C. Crowe, M. Sommerfeld, and Y. Tsuji, *Multiphase Flows with Droplets and Particles* (CRC Press, New York, 1998).
[25] B. H. Xu and A. B. Yu, Chem. Eng. Sci. **52**, 2785 (1997).
[26] R. Y. Yang *et al.*, J. Appl. Phys. **94**, 3025 (2003).
[27] R. P. Zou and A. B. Yu, Chem. Eng. Sci. **51**, 1177 (1996).
[28] J. N. Israelachvili, *Intermolecular and Surface Forces* (Academic, London, 1991).
[29] A. B. Yu *et al.*, Powder Technol. **92**, 185 (1997).
[30] P. Meakin and R. Jullien, Physica (Amsterdam) **187A**, 475 (1992).
[31] A. J. Forsyth *et al.*, Phys. Rev. Lett. **87**, 244301 (2001).
[32] J. M. Valverde *et al.*, Phys. Rev. Lett. **92**, 258303 (2004).
[33] M. Mizuno *et al.*, Kona Powder Part. **9**, 19 (1991).